

Search for Structures in $\bar{p}p$ Total Cross Section below 1 GeV/c

T. Sumiyoshi, J. Chiba, T. Fujii, H. Iwasaki,^(a) T. Kageyama, S. Kuribayashi,
K. Nakamura, and T. Takeda

Department of Physics, University of Tokyo, Tokyo 113, Japan

and

H. Ikeda

National Laboratory for High Energy Physics, Oho, Ibaraki 305, Japan

and

Y. Takada

Institute of Applied Physics, University of Tsukuba, Sakura, Ibaraki 305, Japan

(Received 1 June 1982)

A search has been made for resonant structures with a width greater than 10 MeV/c² in $\bar{p}p$ total cross section between 335 and 960 MeV/c. The measurement has been performed by a transmission method supplemented with proportional chambers and a beam-monitoring spectrometer. No resonant structure has been found, and 90% confidence-level upper limits for the resonant cross sections are presented.

PACS numbers: 13.75.Cs, 14.20.Pt

The $\bar{p}p$ resonances have attracted much interest because, if they exist, they are the best candidates for the exotic hadrons composed of two quarks and two antiquarks.¹ Unfortunately, all the narrow $\bar{p}p$ peaks reported so far¹ have not been confirmed by recent experiments.² However, the broad T and U enhancements observed in $\bar{p}p$ total, elastic, and annihilation cross sections¹ are still candidates for the $\bar{p}p$ resonances. Possible $\bar{p}p$ resonances in this energy region are also reported in the partial-wave analyses^{3,4} of the $\bar{p}p \rightarrow \pi^+\pi^-$ and $\pi^0\pi^0$ reactions though they are not identified as the T or U . It is not clear whether a broad enhancement exists in $\bar{p}p$ total cross section below 1 GeV/c. If the T and U should be genuine resonances, their Regge recurrences would be expected to exist in this region. A hint for the existence of such a broad enhancement has been suggested by Hamilton *et al.*⁵ at 1940 MeV/c².

We have performed an experiment to search for resonant structures in $\bar{p}p$ and $\bar{p}d$ total cross sections at beam momenta between 335 and 960 MeV/c, at the National Laboratory for High Energy Physics (KEK). In this Letter, we report the $\bar{p}p$ results. The present experiment is based on a transmission method, but is characterized by the use of proportional chambers placed in the beam, and a beam-monitoring spectrometer. Since the scintillators cannot be isolated, annihilation of antiprotons in their light guides or in other nearby matter might cause a certain bias in a conventional transmission-counter experi-

ment where no tracking information is available. Also, fluctuation of the phase space and momentum of the beam is dangerous, if not properly monitored. We believe that the present method is more reliable than the conventional transmission method when subtle structures are searched for in the total-cross-section measurement. This technique was first employed in our previous experiment.⁶ In the present experiment, the number of the proportional chambers was increased, and care was taken to reduce nontarget material.

Figure 1 shows the experimental arrangement. Incident antiprotons were momentum analyzed to $\pm 0.5\%$ by a hodoscope H1 placed at an intermediate focus of the partially separated beam line (K3). The absolute momentum was calibrated to $\pm 0.5\%$ by a bending magnet D3 whose magnetic field was accurately measured, and by a hodoscope H3 placed along the focal plane of D3. The point-to-point accuracy of the beam momentum was $\pm 0.05\%$. The target assembly consisted of three Mylar cells, 10 cm in diameter: a 217-mm-long liquid-hydrogen cell, an empty cell having the same structure, and a liquid-deuterium cell. The temperature of the liquids was controlled within ± 0.14 K.

The trajectories of incoming and outgoing charged particles were measured by proportional chambers of bidimensional readout, MWPC1-MWPC4 and MWPC5-MWPC7, respectively. Transmitted antiprotons were detected by a counter C4 which covered a scattering angle region $\theta \lesssim 7^\circ$. Behind C4 there was a hodoscope H2 for

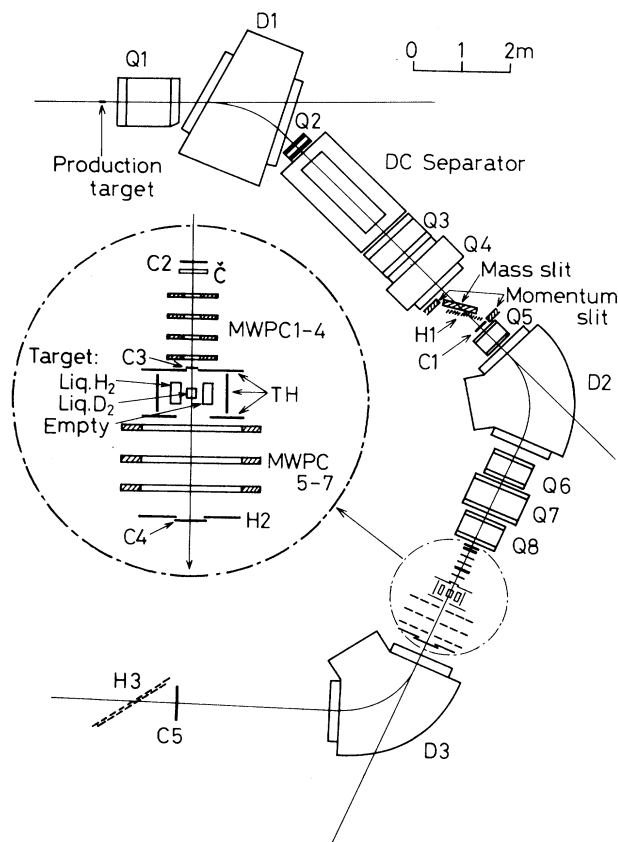


FIG. 1. Experimental arrangement. D1–D3, bending magnet; Q1–Q8, quadrupole magnet; C1–C5, scintillation counters; H1–H3 and TH, scintillator hodoscopes; MWPC1–MWPC7, multiwire proportional chambers; Č, water Čerenkov counter which was only used at high momenta.

the detection of elastically scattered antiprotons.⁷ The pulse-height (dE/dx) information from C4 was used to identify transmitted antiprotons and to reject pions. Additional information for the rejection of the pions from annihilation events came from a scintillation counter hodoscope TH which covered about 96% of the solid angle around the target.

Below 800 MeV/c, the trigger requirement was a threefold coincidence C1 · C2 · C3 timed to the antiprotons, with the thresholds of C1 and C3 set high to reject pions. Further rejection of the beam pions was achieved by an intelligent CAMAC branch driver⁸ at a data-acquisition stage. At higher beam momenta, a water Čerenkov counter (Č) was used to veto the beam pions. Pulse heights of C1–C3 and Č, and time-of-flights (TOF's) between C1 and other trigger counters were recorded for further cleanup of the antiproton selection in the later analysis.

TABLE I. Systematic corrections and uncertainties in millibarns at 500 MeV/c.

Target length	± 0.3
Absolute beam momentum	± 0.5
Pion contamination in the beam	-0.04 ± 0.04
Momentum difference between full- and empty-target runs	-0.61 ± 0.10
Coulomb	-0.23
Coulomb-nuclear interference	-0.16 ± 0.52
Nuclear elastic	6.51 ± 0.10

The measured momentum range was swept in steps of one half of a beam momentum bite of $\pm 2.5\%$. Each datum point was measured three or four times below 800 MeV/c, and twice above 800 MeV/c. Consistency among the different measurements has been proved to be excellent, which means that there were no prominent time-dependent systematic errors. Since the trigger condition was changed, a region around 750 MeV/c of about 50 MeV/c was measured with both trigger conditions for consistency checks.

To obtain the total cross section, we first deduced the partial cross section defined by the transmission counter C4. The transmission ratios of the antiprotons at 500 MeV/c were 85.0% and 98.5% for the full- and empty-target runs, respectively. For those antiprotons which passed through C4 and reached C5, unambiguous identification was possible using TOF between C1 and C5. For other events having a C4 hit by a charged particle, the identification was done based on the dE/dx and TOF from C4, and the MWPC information when necessary. Unambiguous identification was also possible for those events with no TH or H2 hit and having dE/dx and TOF from C4 consistent with the antiproton. If there was a TH hit in addition to the C4 hit, it was either due to the antiproton annihilation in the target region, or due to an accidental TH hit. If a slow, highly ionizing pion coming from the annihilation hits C4, the multiplicity of TH tends to be more than 1. By this TH multiplicity criteria, most slow pions which faked antiprotons could be rejected. Also the tracking information was helpful to recognize the accidental TH hits. Some events had an H2 hit in addition to the C4 hit. Dangerous background in this category of events is the annihilation of antiprotons near C4 followed by a slow-pion or multipion hit of C4. Such events were rejected by examining the tracking information of the outgoing antiproton. Because of a slight reconstruction inefficiency, a certain num-

ber of events belonging to this category had to be treated statistically. This introduced an uncertainty of $\pm(0.2-0.4)$ mb in addition to that arising from pure counting statistics, $\pm(0.4-0.6)$ mb. A quadratic sum of these uncertainties represents the point-to-point error. Other systematic corrections and their uncertainties, typically at 500 MeV/c, are listed in Table I. They contribute to the overall normalization error of ± 1 mb.

The total cross section has been obtained from the partial cross section after the corrections for the Coulomb, Coulomb-nuclear interference, and nuclear elastic terms integrated outside and inside of the acceptance of the counter C4. For these corrections the real-to-imaginary ratio of the $\bar{p}p$ forward amplitude and the slope parameter of the diffraction peak of $\bar{p}p$ elastic scattering were taken from previous results.⁹ Since the correction terms include the total cross section itself, we started with the partial cross section and the corrections were iterated until the resulting total cross section converged.

The results are shown in Fig. 2 where the circles and triangles represent the data taken with the trigger conditions $C1 \cdot C2 \cdot C3$ and $C1 \cdot C2 \cdot C3 \cdot \bar{C}$, respectively. At the bottom of this figure is shown the momentum or mass resolution, which

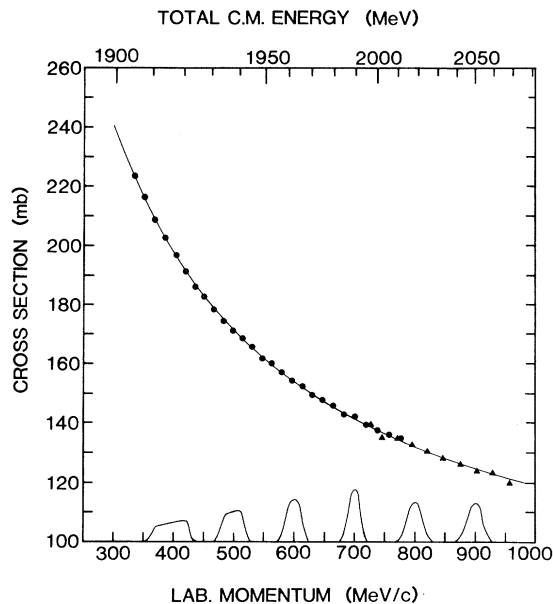


FIG. 2. The results for $\bar{p}p$ total cross section. The filled circles and triangles represent different trigger conditions. The curve shows the result of the fit with $\sigma_{tot} = a + b/p$. The momentum resolution is indicated at the bottom.

is mainly determined by the energy loss in the target at low momenta, and by the momentum spread of the beam at high momenta. The root mean square mass resolution around 1940 MeV/ c^2 is 3 MeV/ c^2 . The momentum (p) corresponding to each datum point is a mean of the resolution function weighted by the total cross section (σ_{tot}), where the attenuation in the target is also taken into account. The curve in Fig. 2 is the result of the fit with a functional form $\sigma_{tot} = a + b/p$, where $a = 66.5$ mb and $b = 52\,454$ mb MeV/ c with $\chi^2 = 51.0$ for 34 degrees of freedom (DF). Figure 3 shows the difference between the data points and the fitted curve. The error bars represent the point-to-point errors. The solid curve shows the effect of the narrow S resonance reported by Carroll *et al.*¹⁰ and the dashed curve shows that of the broad S suggested by Hamilton *et al.*⁵ To calculate these curves, the mass resolution was taken into account. The fits to the data with a functional form $\sigma_{tot} = a + b/p + (\text{Breit-Wigner resonance term})$ give $\chi^2 = 1753$ with the resonance parameters given by Carroll *et al.*,¹⁰ and $\chi^2 = 179$ with those given by Hamilton *et al.*,⁵ for DF = 34. From these results, the nonexistence of

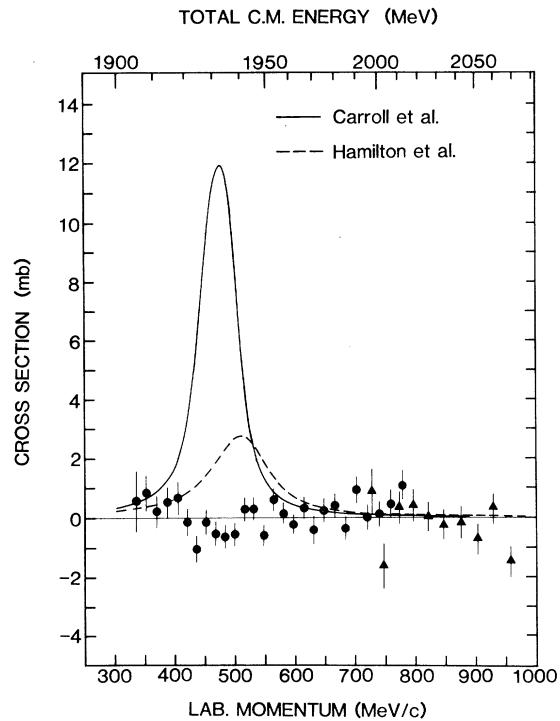


FIG. 3. The total cross section data plotted after subtraction of the fitted curve, and compared with the S -resonance contribution reported by some experiments.

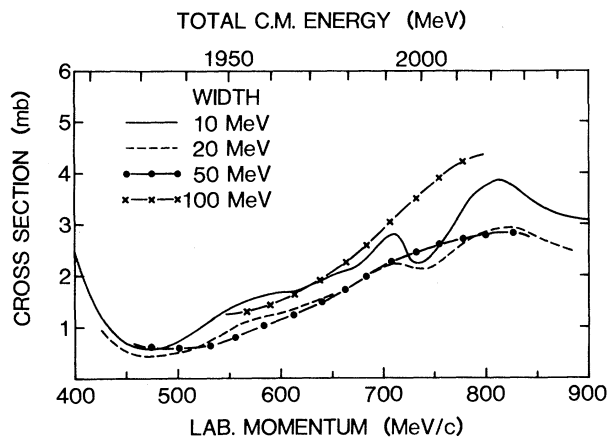


FIG. 4. 90%-confidence-level upper limits for possible resonances.

the narrow S reported by Carroll *et al.*¹⁰ is reconfirmed, and the broad S reported by Hamilton *et al.*⁵ is rejected at a confidence level of more than 99%. Finally, we have calculated 90%-confidence-level upper limits of resonance cross sections for given mass and width (≥ 10 MeV/ c^2) parameters. The results are presented in Fig. 4.

To conclude, no significant resonant structure with a width of more than 10 MeV/ c^2 has been found in our measurement. In particular, it should be noted that below 500 MeV/ c , our data show much smoother behavior than the previous data.^{5,10} This is partly because our data have improved statistical accuracy there. However,

it is more likely that at very low momenta, our method allows more reliable total-cross-section measurement than the conventional transmission method.

We are grateful to the staff of the National Laboratory for High Energy Physics for excellent machine operation and technical assistance. We wish to acknowledge many stimulating discussions with Professor T. Kamae. This work was supported in part by a Grant in Aid from the Japanese Ministry of Education, Science, and Culture.

^(a)Present address: Lawrence Berkeley Laboratory, Berkeley, Cal. 94720.

¹L. Montanet *et al.*, Phys. Rep. **63**, 149 (1980).

²T. Kamae, Nucl. Phys. **A374**, 25c (1982).

³A. D. Martin and M. R. Pennington, Nucl. Phys. **B169**, 216 (1980).

⁴B. R. Martin and D. Morgan, Nucl. Phys. **B176**, 355 (1980).

⁵R. P. Hamilton *et al.*, Phys. Rev. Lett. **44**, 1182 (1980).

⁶T. Kamae *et al.*, Phys. Rev. Lett. **44**, 1439 (1980).

⁷The results of elastic scattering are being analyzed.

⁸KEK standard, CCS-11 (CAMAC Control Subsystem). It is a 16-bit microcomputer with 48-kbyte memory.

⁹H. Iwasaki *et al.*, Phys. Lett. **103B**, 247 (1981); J. E. Enstrom *et al.* (Particle Data Group), Lawrence Berkeley Laboratory Report No. LBL-58, 1972 (unpublished).

¹⁰A. S. Carroll *et al.*, Phys. Rev. Lett. **32**, 247 (1974).